used as data, but only in obtaining the starting values. Note that this method can give values of the coefficients that best fit any *given* fairing of the experimental data. To modify this fairing of the data and obtain a better fit requires the parametric differentiation technique described in this paper.

References

[1] Nicolaides, J. D., "On the Free-Flight Motion of Missiles Having Slight Configurational Asymmetries," BRL Rept. 858, AD 27405, 1953, Ballistic Research Labs., Aberdeen Proving Ground, Md.

[2] Malcolm, G. N. and Chapman, G. T., "A Computer Program for Systematically Analyzing Free-Flight Data to Determine the Aerodynamics of Axisymmetric Bodies," TN D-4766, 1968, NASA.

[3] Murphy, C. H., "Free-Flight Motion of Symmetric Missiles," BRL Rept. 1216, AD 442757, 1963, Ballistic Research Labs., Aberdeen Proving Ground, Md.

[4] Rasmussen, M. L. and Kirk, D. B., "On the Pitching and Yawing Motion of a Spinning Symmetric Missile Governed by an Arbitrary Nonlinear Restoring Moment," TN D-2135, 1964, NASA.

[5] Bellman, R., Kagiwada, H., and Kalaba, R., "Quasilinearization, System Identification, and Prediction," RM-3812-PR, 1963, RAND Corp., Santa Monica, Calif.

[6] Goodman, T. R., "System Identification and Prediction—An Algorithm Using a Newtonian Iteration Procedure," *Quarterly of Applied Mathematics*, Vol. XXIV, No. 3, Oct. 1966, pp. 249–255.

[7] Rubbert, P. E. and Landahl, M. T., "Solution of the Transonic Airfoil Problem through Parametric Differentiation," *AIAA Journal*, Vol. 5, No. 3, March 1967, pp. 470–479.

[8] Kruse, R. L., Malcolm, G. N., and Short, B. J., "Comparison of Free-Flight Measurements of Stability of the Gemini and Mercury Entry Capsules at Mach Numbers 3 and 9.5," TM X-957, 1964, NASA.

[9] Boissevain, A. G. and Intrieri, P. F., "Determination of Stability Derivatives From Ballistic Range Tests of Rolling Aircraft Models," TM X-399, 1961, NASA.

APRIL 1970 AIAA JOURNAL VOL. 8, NO. 4

A Transformation Theory for the Compressible Turbulent Boundary Layer with Mass Transfer

CONSTANTINO ECONOMOS*
General Applied Science Laboratories Inc., Westbury, N. Y.

The problem of the turbulent boundary layer with variable fluid properties and transpiration at constant pressure has been treated by modification and extension of the Coles' compressibility transformation. This analysis has been applied to several cases involving mass transfer both with and without chemical reactions. Comparison of these results with experiment has shown they yield more accurate predictions for gross boundary-layer properties than those obtained using earlier analyses. In addition, detailed analysis of velocity profiles has shown that the transformation correctly maps the "law of the wall" region to a constant property form. However, in complete analogy with the behavior observed by Baronti and Libby for the high-speed impermeable case, it is found that the transformation distorts the wake region of the profiles in the sense that the flat plate value of the Coles' wake parameter Π is not recovered. The magnitude of this distortion is shown to be roughly correlated by the density ratio ρ_w/ρ_e across the boundary layer.

Nomenclature

$c_f,\bar{c}_f$ = local skin-friction coefficients
$F,\bar{F}$ = $\rho_w v_w/\rho_e u_e$, $\bar{\rho}\bar{v}_w/\bar{\rho}\bar{u}_e$
k_1,k_2 = law of the wall constants, Eq. (21)
M = Mach number
$R_x,R_{\bar{x}}$ = Reynolds numbers based on $x,\bar{x}$
$R_y,R_{\bar{y}}$ = Reynolds numbers based on $y,\bar{y}$
$R_\delta,R_{\bar{\delta}}$ = Reynolds numbers based on $\delta,\bar{\delta}$
$R_\vartheta,R_{\bar{\vartheta}}$ = Reynolds numbers based on $\theta,\bar{\theta}$
T,T_t = temperature, total temperature
$u,\bar{u}$ = streamwise velocity components
$\bar{U}$ = $(2\bar{c}_f)^{1/2}[(1 + 2\bar{F}\bar{u}/\bar{c}_f)^{1/2} - 1]/\bar{F}$
$v,\bar{v}$ = normal velocity components
w = functional form = $2\alpha^2(3 - 2\alpha)$
W = molecular weight
$x,\bar{x}$ = streamwise coordinates
$y,\bar{y}$ = normal coordinates
Y = mass fraction
α = $R_{\bar{y}}/R_{\bar{\delta}}$
$\delta,\bar{\delta}$ = boundary-layer thicknesses
$\zeta,\bar{\zeta}$ = $2F/c_f, 2\bar{F}/\bar{c}_f$
η,ξ,σ = parameters of the transformation
$\theta,\bar{\theta}$ = momentum thicknesses
$\mu,\bar{\mu}$ = coefficients of viscosity
Π = Coles' wake parameter, Eq. (22)
$\rho,\bar{\rho}$ = densities
$\tilde{\sigma}$ = $\sigma\mu_e/\bar{\mu}$
$\tau,\bar{\tau}$ = shear stresses (including Reynolds stresses)
Φ = $\Phi = (\pi/k_1)(2 - w) - (1/k_1)\ln\alpha$
χ,χ = Reynolds numbers based on distance from arbitrary initial station
$\psi,\bar{\psi}$ = stream functions

Presented as Paper 69-161 at the AIAA 7th Aerospace Sciences Meeting, New York, January 20–22, 1969; submitted January 24, 1969; revision received August 21, 1969. Taken in part from the author's Ph.D. dissertation in the Polytechnic Institute of Brooklyn, Department of Aeronautics and Astronautics. This work was supported in part by NASA Contract NAS8-2686 and ARPA Contract DA-49-0830SA-3135. The author gratefully acknowledges the guidance and encouragement of P. Libby, University of California, San Diego.

* Supervisor, Thermochemistry and Viscous Flow Section. Member AIAA.

Subscripts

e = external conditions
s = sublayer edge conditions
w = wall conditions
$(\ )$ = variables in the VP flow
$(\bar{\ })$ = variables in the CP flow
$(\tilde{\ })$ = normalization with respect to corresponding external value, e.g., $\tilde{u} = u/u_e$

I. Introduction

In a variety of applications associated with high-performance atmospheric flight the problem of protecting vehicle surfaces from intense aerodynamic heating rates is encountered. Among the more effective techniques for providing this protection are those which are characterized by a nonzero normal velocity component at a solid surface, i.e., subliming ablation and transpiration. As a result of this mass transfer and the associated surface roughness it can be anticipated that the state of the boundary layer will be turbulent. Accordingly, an understanding of the behavior of the variable property (VP) turbulent boundary layer with mass transfer is of considerable practical interest.

Existing theories[1-6] which treat this flow configuration provide rough estimates of gross boundary-layer properties such as skin friction and (steady-state) recession rates. However, they do not provide the detailed profile information required for an accurate description of the phenomenon since each of them utilizes arbitrary extrapolations of the phenomenology developed for the low-speed, constant property (CP) case. In this paper a new phenomenological treatment is developed which improves this representation by utilizing the concept of a "compressibility" transformation to relate the flowfield of interest to a companion CP flow. Thus, this formulation is a generalization of the analysis of Baronti and Libby[7] who treated the high-speed impermeable case by applying the transformation theory of Coles.[8]

The advantage of the approach proposed here resides in the fact that no arbitrary assumptions regarding the behavior of turbulent momentum transport in the VP flowfield is required. Instead, it is only necessary to specify this behavior for the CP flow for which, at least from a phenomenological point of view, an adequate description is currently available. Of course, implementation of this method is not possible without a suitable CP formulation. In the present analysis the method due to Stevenson[9,10] is utilized for this purpose and is described briefly in Secs. II and III.

Finally, it is emphasized here that the basic objective in the present paper is development of a more accurate analytic description of the velocity field. Thus, the energy and species solutions which are needed to complete the describing equations are not considered in great detail. In general, it is assumed that the thermodynamics of the VP flow can be related to the velocity field. Suitable Crocco relations are utilized to provide the required numerical values. For each of the cases for which predictions are presented here it is shown that the Crocco integral is a reasonably valid approximation.

II. Theoretical Considerations†

Fundamental Transformation Relations

The describing differential equations for the velocity field of interest here are assumed to be of the form

$$\partial\rho u/\partial x + \partial\rho u/\partial y = 0 \tag{1}$$

$$\rho u\partial u/\partial x + \rho v\partial u/\partial y = \partial\tau/\partial y \tag{2}$$

† Only a brief outline of the formal development is presented here. For more detailed derivations see Ref. 11.

It can be shown that this system of equations can be transformed identically to the CP form

$$\partial\bar{u}/\partial\bar{x} + \partial\bar{v}/\partial\bar{y} = 0 \tag{3}$$

$$\bar{\rho}\bar{u}\partial\bar{u}/\partial\bar{x} + \bar{\rho}\bar{v}\partial\bar{u}/\partial\bar{y} = \partial\bar{\tau}/\partial\bar{y} \tag{4}$$

by introduction of the following transformation relations‡:

$$d\bar{x}/dx = \xi(x) \tag{5}$$

$$\bar{\rho}d\bar{y}/\rho dy = \eta(x) \tag{6}$$

$$(\bar{\psi} - \bar{\psi}_w)/(\psi - \psi_w) = \sigma(x) \tag{7}$$

provided that the following correspondences between gross boundary-layer parameters are imposed:

$$\sigma/\eta = \text{constant} = \bar{u}_s/u_e \tag{8}$$

$$u/u_e = \bar{u}/\bar{u}_e \equiv \tilde{u} \tag{9}$$

$$dR_\theta/d\chi = F + c_f/2 \tag{10}$$

$$dR_{\bar{\theta}}/d\chi = \bar{F} + \bar{c}_f/2 \tag{11}$$

$$c_f/\bar{c}_f = \tilde{\rho}_w\tilde{\mu}_w\tilde{\sigma}_w \tag{12}$$

$$R_\theta/R_{\bar{\theta}} = 1/\tilde{\sigma} \tag{13}$$

$$R_\delta = \left(\frac{1}{\tilde{\sigma}}\right)\int_0^{R_{\bar{\delta}}} \frac{dR_{\bar{y}}}{\tilde{\rho}} \tag{14}$$

Here the existence of mass transfer in both flow regimes is manifested by the presence of the terms $F \equiv \rho_w v_w/\rho_e u_e$ and $\bar{F} \equiv \bar{\rho}\bar{v}_w/\bar{\rho}\bar{u}_e$.

Following Stevenson[9,10] the CP variables are taken to be related by

Velocity profiles:

$$\tilde{u} = \begin{cases} (2\bar{F}/\bar{c}_f)[\exp(\bar{F}R_{\bar{y}}) - 1]; & 0 \le R_{\bar{y}} \le R_{\bar{y}_s} \\ 1 - (\bar{F} + \bar{c}_f/2)^{1/2}\Phi + 0.25\bar{F}\Phi^2; & R_{\bar{y}_s} < R_{\bar{y}} \le R_\delta \end{cases} \tag{15}$$

Skin-friction law:

$$\ln(R^2_{\bar{\delta}}\bar{c}_f/2)^{1/2} = k_1\{(2/\bar{F})(2/\bar{c}_f)^{1/2}[(1 + 2\bar{F}/\bar{c}_f)^{1/2} - 1] - k_2 - 2\pi/k_1\} \tag{16}$$

Momentum thickness:

$$R_{\bar{\theta}}/R_{\bar{\delta}} = (\bar{c}_f/2)^{1/2}(1 + 2\bar{F}/\bar{c}_f)^{1/2}(I_1 + 0.5\bar{F}I_3) - (\bar{c}_f/2)(1 + 2\bar{F}/\bar{c}_f)^{1/2}I_2 - \bar{F}(I_2 + 0.25\bar{F}I_4) \tag{17}$$

Sublayer Reynolds number:

$$\exp[(\bar{F}^2/2\bar{c}_f)^{1/2}(R_{\bar{y}_s}{}^2\bar{c}_f/2)^{1/2}] - (1/k_1)(\bar{F}^2/2\bar{c}_f)^{1/2}\ln(R_{\bar{y}_s}{}^2\bar{c}_f/2)^{1/2} = 1 + k_2(\bar{F}^2/2\bar{c}_f)^{1/2} \tag{18}$$

where

$$I_1 = k_1{}^{-1}(\Pi + 1),\ I_2 = k_1{}^{-2}(1.49\Pi^2 + 3.17\Pi + 2)$$

$$I_3 = k_1{}^{-3}(2.46\Pi^3 + 8.3\Pi^2 + 11\Pi + 6)$$

$$I_4 = k_1{}^{-4}(4.27\Pi^4 + 20.1\Pi^3 + 41.7\Pi^2 + 46.6\Pi + 24)$$

and k_1 and k_2 are the usual log law constants for impermeable CP flow. (The values utilized in the present calculations are $k_2 = 4.9$, $1/k_1 = 2.43$.) Note that (18) implies that the quantity $(R_{\bar{y}_s}{}^2\bar{c}_f)^{1/2}$ is not a constant as in the impermeable case,§ but varies with the local blowing intensity. Note also

‡ It is noted here that (7) represents a modification of the original Coles' stretching. The significance and motivation for this modification is discussed in Ref. 11. Here we note only that (7) follows directly from the definition of the stream functions and (6) and (9) when ψ_w and $\bar{\psi}_w$ are nonzero.

§ For $\bar{F} = 0$ the constants utilized here imply $(R_{\bar{y}_s}{}^2\bar{c}_f/2)^{1/2} = 10.6$. See Ref. 11 for graphical representation of (18) when $\bar{F} \neq 0$.

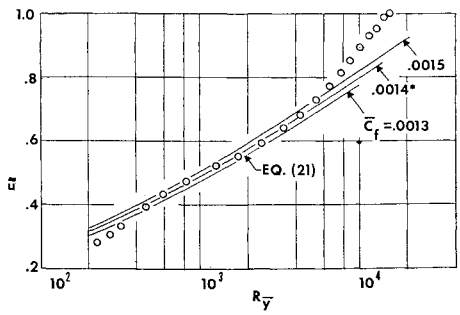

Fig. 1 Estimate of CP skin-friction coefficient from transpired velocity profile data—typical result:[15] run A-18, $R_{\bar{\theta}} = 2400$, $\bar{F} = 0.0036$; selected value of $\bar{c}_f$ has been indicated by an asterisk.

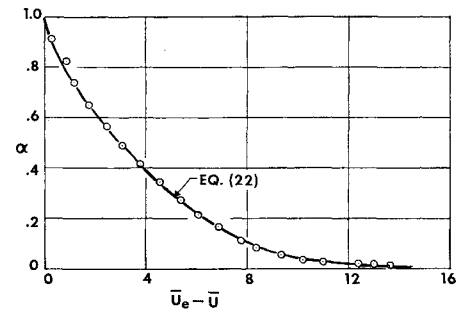

Fig. 3 Comparison of velocity defect law Eq. (22) with transpired velocity profile data—typical result;[15] run A-18, $R_{\bar{\theta}} = 2400$, $\bar{F} = 0.0036$.

that (15–17), when combined with the CP momentum integral (11), permit determination of the streamwise boundary-layer development when the blowing intensity $\bar{F}$ is prescribed. Here, of course, this parameter is considered to be an unknown, as will be indicated below.

Completion of the System of Working Equations

If it is assumed that $\bar{F}$ is a prescribed function of the VP Reynolds number χ and that the thermodynamics can be related to the velocity field by means of a Crocco integral, (8–17) constitutes a system of 7 equations for 9 dependent variables (R_θ, $R_{\bar{\theta}}$, R_δ, $R_{\bar{\delta}}$, c_f, $\bar{c}_f$, $\bar{F}$, $\tilde{\sigma}$, χ) with the CP Reynolds number $\bar{\chi}$ the sole independent variable. Accordingly, two additional equations are required. One is obtained by invoking the sublayer hypothesis which can be written[7,11]

$$\tilde{\sigma} = \left(\frac{\tilde{\rho}_s}{\tilde{\mu}_s R_{\bar{y}_s}}\right) \int_0^{R_{\bar{y}_s}} \frac{dR_{\bar{y}}}{\tilde{\rho}} \tag{19}$$

In view of the assumptions made earlier this is an implicit relation of the form

$$\tilde{\sigma} = \tilde{\sigma}(R_{\bar{y}_s}, R_{\bar{\delta}}, \bar{c}_f, \bar{F})$$

or in view of (18)

$$\tilde{\sigma} = \tilde{\sigma}(R_{\bar{\delta}}, \bar{c}_f, \bar{F}) \tag{19a}$$

The final equation is obtained by satisfying the first wall compatibility condition in both flow regimes, i.e., we satisfy the momentum equations (2) and (4) at $y, \bar{y} \to 0$ taking into account the differentiation rules implied by the transformation and that

$$\tau \to \mu \partial u/\partial y, \ \tilde{\tau} \to \tilde{\mu} \partial \tilde{u}/\partial \bar{y}, \text{ at } y, \bar{y} \to 0$$

As a result of this procedure there is obtained

$$2\bar{F}/\bar{c}_f = 2F/c_f - (\partial \ln \tilde{\rho}\tilde{\mu}/\partial \tilde{u})_w \tag{20}$$

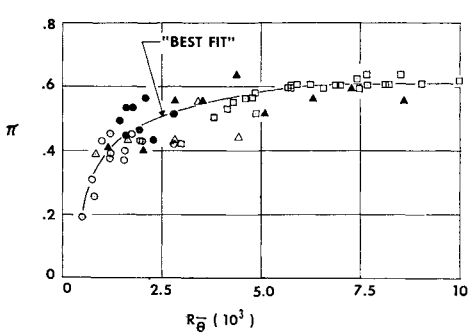

Fig. 2 Magnitude of wake component in CP flows with and without transpiration: $\bar{F} = 0$ for open symbols, $\bar{F} \neq 0$ for solid symbols; squares, Ref. 14; circles, Ref. 15; triangles, Ref. 20.

Note that in the case of homogeneous injection at adiabatic wall conditions (20) implies the invariance under the transformation of the blowing parameter ζ. A similar conclusion holds for the case $\tilde{\rho}\tilde{\mu} = \text{const}$. However, note that for heterogeneous injection this situation is not likely to arise.

III. Comparison of Theory and Experiment for the CP Case

In order to assess the adequacy of the CP formulation utilized here an extensive comparison with the available experimental data was conducted.[11] Some representative results of this investigation are shown in Figs. 1–3. In Fig. 1 the inner region of the velocity field is compared with the law of the wall portion of the assumed velocity variation. The latter can be written as

$$\tilde{u} = k_2[(\bar{c}_f/2)^{1/2} + k_2\bar{F}/4] + (1/2k_1)[(\bar{c}_f/2)^{1/2} + k_2\bar{F}/2] \times \ln(R_{\bar{y}^2}\bar{c}_f/2) + (\bar{F}/16k_1^2)[\ln(R_{\bar{y}^2}\bar{c}_f/2)]^2 \tag{21}$$

For the value of $\bar{F}$ indicated in this figure, Eq. (21) was utilized to generate several curves corresponding to different choices of the skin-friction coefficient $\bar{c}_f$. In this manner the value which best correlates the data can be established yielding an "experimental" determination of the skin friction. This procedure was first utilized by Clauser[12] for the low-speed impermeable case. It is evident from the results shown that an unambiguous selection of $\bar{c}_f$ can be made. Furthermore, the general agreement of the theoretical curves with the data points verifies to some extent that the constants k_1 and k_2 are unaffected by transpiration as is assumed in the derivation of (21).

For the outer region of the transpired velocity profile a "defect law" can be formulated as for the impermeable case and can be written

$$\tilde{U}_e - \tilde{U} = (\Pi/k_1)[2 - w(\alpha)] - \ln\alpha \tag{22}$$

where Π and $w(\alpha)$ are the Coles' wake parameter and the Coles' wake function, respectively.[13] Again both of these are assumed to take on impermeable values even with transpiration. The validity of these assumptions was also examined in Ref. 11 as follows. Once the values of $\bar{F}$, $\bar{c}_f$, and $R_{\bar{\delta}}$ for a particular profile have been established the value of Π implied by (16) can be determined. This was done for a number of cases as shown in Fig. 2 where transpired results have been compared with similar data obtained from impermeable flows.[14] It is clear that there is no trend indicated which can be associated with transpiration as such. However, a tendency for Π to approach zero at low values of the momentum thickness Reynolds number is apparent for both the zero and nonzero cases. This observation has previously been made by Coles.[8] Finally, the invariance of the wake function $w(\alpha)$ with transpiration is demonstrated by the representative result shown in Fig. 3.

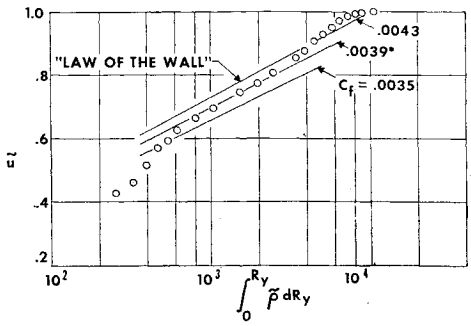

Fig. 4 Estimate of VP skin-friction coefficient from transpired velocity profile data—typical result with helium injection;[15] run H-3, Table 1.

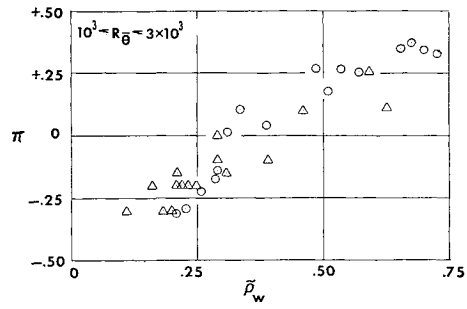

Fig. 5 Variation of Coles' wake parameter with density ratio; circles, low-speed helium injection results;[15] triangles, high-speed impermeable results.[7]

IV. Comparison of Theory and Experiment for the VP Case

Low-Speed Helium Injection

The flow configuration here is that of a boundary layer on a porous circular cylinder with transpiration of helium into a low speed ($M_e \approx 0.1$) air stream.[15] The data which is available includes velocity, temperature, and concentration profiles with four different rates of uniform injection in the range $0.00022 \leq F \leq 0.0014$. These profiles were obtained at several streamwise stations along the axis of the cylinder yielding a relatively small but significant Reynolds number variation of $0.25 \times 10^6 \leq \chi \leq 0.8 \times 10^6$ based on distance measured from the origin of transpiration. A detailed examination of the temperature and concentration profiles indicated that the boundary layer was essentially isothermal and that the concentration of helium varied linearly with $\tilde{u}$ from the wall value to zero at the outer edge. Accordingly, the density distribution which appears in (19) and (20) was taken to be

$$(1/\tilde{\rho}) = 1 + Y_{\mathrm{He}_w}(W_{\mathrm{air}}/W_{\mathrm{He}} - 1)(1 - \tilde{u})$$

where Y_{He_w} denotes the local wall concentration of helium as determined experimentally. The viscosity of the mixture was determined from the local concentration using the relation for a binary mixture given in Ref. 16.

As a first step in analyzing these results the value of c_f for each of the available profiles was determined in a manner similar to that described in a previous section. This involves selection of several values of c_f and the corresponding values of $\bar{F}$ and $\bar{c}_f$ and $\tilde{\sigma}$ which satisfy Eqs. (12), (19), and (20). One can then generate the velocity profile (in the inner region) in the form $\tilde{u} = \tilde{u}(R_{\tilde{y}}/\tilde{\sigma})$ by use of Eq. (21). Since

$$R_{\tilde{y}}/\tilde{\sigma} \equiv \int_0^{R_y} \tilde{\rho} dR_y$$

[c.f., Eq. (14)] and $\tilde{u}(R_y)$ and $\tilde{\rho}(R_y)$ are known experimentally, the value of c_f which best correlates the profiles can be selected. Furthermore, by utilizing (16) the value of Π in the transformed plane can also be deduced.

This procedure has been applied to the sixteen profiles presented in Ref. 15 and the results are summarized in Table 1. One of the generalized Clauser plots used to obtain estimates of the skin friction is shown in Fig. 4 where the estimated value of c_f has been indicated by an asterisk. Evidently, the law of the wall portion of the profiles is well correlated by this procedure.

An interesting result of this profile analysis is the behavior of the parameter Π as determined from (16). As may be seen in Table 1, a systematic decrease with increasing injection rate is observed. This result is analogous to that obtained by Baronti and Libby[7] in connection with an analysis of velocity profiles on an impermeable flat plate at high speed ($1.7 \leq M_e \leq 9$). In this case, Π was found to decrease more or less systematically with increasing Mach number. This similarity in behavior is demonstrated graphically in Fig. 5. Here an attempt has been made to correlate the variation of Π with the density ratio across the boundary layer. Although not completely satisfactory, some correlation is evident.

Utilizing this correlation and the system of equations described previously, predictions for the streamwise variation of skin friction and momentum thickness were generated. A representative comparison with experiment is shown in Fig. 6. The corresponding velocity profiles as obtained from this integration are also compared with experiment in Fig. 7. Evidently, the agreement which is obtained is excellent in all respects.

Finally, a comparison of the prediction of the present method and that of Ref. 2 is shown in Fig. 8, where the net reduction in skin-friction coefficient has been plotted vs the blowing parameter ζ. The superiority of the present method is clearly evident.

Table 1 Summary of profile parameters deduced from results of Ref. 15[a]

Run no.	F[b] (+3)	Y_{He_w}	c_f* (+3)	$\bar{c}_f$ (+3)	$\bar{F}$ (+3)	R_θ (−3)	Π	χ (−6)
H3	0.22	0.058	3.9	4.8	−0.29	0.94	0.33	0.26
H4	0.22	0.065	3.6	4.4	−0.25	1.30	0.35	0.44
H5	0.22	0.075	3.4	4.4	−0.34	1.50	0.37	0.61
H6	0.22	0.083	3.1	4.2	−0.34	2.02	0.35	0.79
H7	0.43	0.116	3.4	4.9	−0.30	0.89	0.26	0.26
H8	0.43	0.135	3.0	4.5	−0.28	1.30	0.27	0.44
H9	0.43	0.149	3.0	4.8	−0.36	1.53	0.18	0.60
H10	0.43	0.164	2.6	4.3	−0.26	1.90	0.27	0.77
H11	0.89	0.245	2.3	4.6	0.46	0.93	0.04	0.25
H12	0.89	0.303	1.8	4.1	0.72	1.26	0.10	0.42
H13	0.89	0.345	1.6	3.9	0.85	1.55	0.01	0.59
H14	0.89	0.382	1.5	3.9	0.95	1.87	−0.14	0.75
H15	1.37	0.385	1.5	3.8	2.08	0.92	−0.18	0.25
H16	1.37	0.460	1.1	3.2	2.79	1.28	−0.23	0.41
H17	1.37	0.533	0.83	2.7	3.41	1.63	−0.30	0.57
H18	1.37	0.600	0.70	2.5	3.91	1.85	−0.32	0.73

[a] Isothermal helium injection with $M_e \approx 0.1$.
[b] Numbers in parenthesis denote powers of 10.

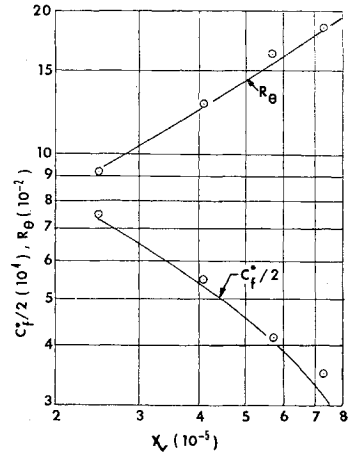

Fig. 6 Comparison of theory and experiment for streamwise variation of skin friction and momentum thickness Reynolds number: solid line, theoretical prediction; circles, data of Ref. 15 with helium injection at $F = 0.00137$.

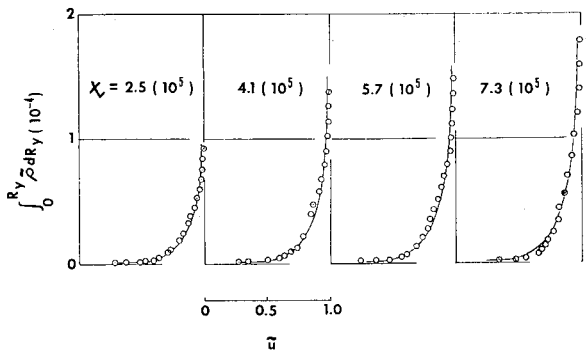

Fig. 7 Comparison of theory and experiment for streamwise velocity profile development: solid line, theoretical prediction; circles, measurements of Ref. 15 with helium injection at $F = 0.00137$.

High-Speed Homogeneous Injection

In this case, the flow configuration consisted of a flat, porous region located downstream of an impermeable flat plate which extended upstream through the throat of a supersonic nozzle.[17] Nitrogen gas, heated sufficiently to obtain an adiabatic wall condition at the porous surface, was injected into a Mach 3.2 external air stream. The distance from the throat to the leading edge of the porous region was approximately 2 ft while the point at which the skin-friction measurements were made was located about 1 ft farther downstream. The skin-friction measurements were made directly by utilizing a skin-friction balance. Measurements were obtained at several rates of injection and at two unit Reynolds number levels. The resulting values of skin-friction coefficient are summarized in Table 2.

In the absence of any profile measurements, the density distribution was taken to be that corresponding to a Crocco integral, i.e., $1/\tilde{\rho} = \tilde{T}_w + (\tilde{T}_{t_e} - \tilde{T}_w)\tilde{u} + (1 - \tilde{T}_{t_e})\tilde{u}^2$. This is a reasonable approximation particularly for the adiabatic wall case involved here.

In order to generate predictions the system of equations was integrated from a "leading edge" with the blowing parameter held fixed at various values corresponding to the experimental conditions. The resulting variation of c_f is shown in Fig. 9. Then an "effective origin" for each of the runs was established by taking into account the impermeable region upstream of the porous plate. This is accomplished by first locating the virtual origin for the $\zeta = 0$ case by utilizing the corresponding value of R_θ, which was experimentally determined to be 33,400. The effective origin for the various blowing cases is then established by assuming the momentum thickness Reynolds number to be continuous across the discontinuity existing at the origin of injection. A crude rationale for this hypothesis follows from (10) if it is assumed to hold in the arbitrarily small region Δx within which the (finite) discontinuity occurs. In this case; (10) may be written

$$\Delta\theta = (c_f/2 + F)\Delta x$$

then, since c_f and F remain finite across the discontinuity,

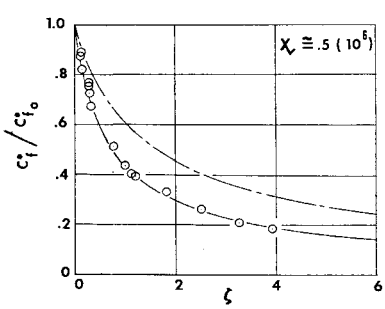

Fig. 8 Comparison of theory and experiment for low-speed helium injection: solid line, present prediction; broken line, prediction of Ref. 2; circles, data of Ref. 15.

Table 2 Summary of skin-friction results of Ref. 17[a]

F^b (+3)	c_f (+3)	ζ	c_f/c_{f_0}
	A. Series I[c]		
0.21	0.69	0.6	0.77
0.40	0.57	1.4	0.64
0.51	0.51	2.0	0.57
0.55	0.50	2.2	0.55
0.63	0.43	2.9	0.48
0.81	0.35	4.6	0.39
0.92	0.30	6.2	0.33
0.98	0.29	6.7	0.33
1.02	0.29	7.1	0.32
1.06	0.24	8.7	0.27
1.19	0.22	10.6	0.25
1.36	0.22	12.6	0.24
1.40	0.15	18.3	0.17
1.41	0.23	12.0	0.26
	B. Series II[d]		
0.20	0.58	0.69	0.74
0.43	0.40	2.12	0.51
0.65	0.28	4.65	0.36

[a] Adiabatic nitrogen injection at $M_e = 3.2$.
[b] Numbers in parenthesis denote powers of 10.
[c] Based on Fig. 14 of Ref. 17 with $c_{f_0} = 0.0009$.
[d] Based on Fig. 12 of Ref. 17 with $c_{f_0} = 0.000785$.

we obtain $\Delta\theta \to 0$ as $\Delta x \to 0$, which implies continuity of θ and R_θ if the external conditions are considered to be unaffected by the transpiration.

In Fig. 10 the variation of the effective origin with ζ as determined by this method has been shown superimposed on the basic c_f vs R_x plot. Note that this locus of points remains close to lines of constant R_θ. This trend is associated with small values of ΔR_x relative to R_{x_0} where ΔR_x represents the extent of the porous region upstream of the point of interest and R_{x_0} represents the length of the impermeable region preceding injection. Actually it can be demonstrated that for $\Delta R_x/R_{x_0} \to 0$ the trace of the effective R_x is coincident with lines of constant R_θ.

The predictions obtained in this manner are compared with the experimental results in Figs. 11 and 12. In Fig. 11 the comparison is made in absolute terms and it is evident that good agreement is obtained. In Fig. 12 these results are presented in terms of net skin-friction reduction along with several other curves corresponding to 1) the prediction that the present analysis would yield if the effect of injection on the virtual origin were not accounted for, i.e., with R_x = const.; 2) the prediction of Rubesin's analysis[3] including the virtual origin effect; and 3) the experimental results obtained by Pappas and Okuno at Mach 3.2.[18]

These comparisons demonstrate the improvement which is obtained when due account of the impermeable region is taken. It also appears that the present method is superior to the earlier analysis of Rubesin. Finally, it is interesting to note the disparity between the two sets of experimental results which were obtained at nominally identical Mach num-

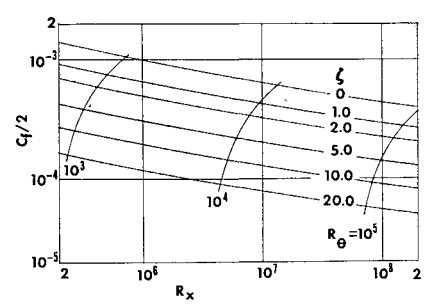

Fig. 9 Streamwise variation of local skin-friction coefficient with homogeneous transpiration; $M_e = 3.2$, adiabatic wall.

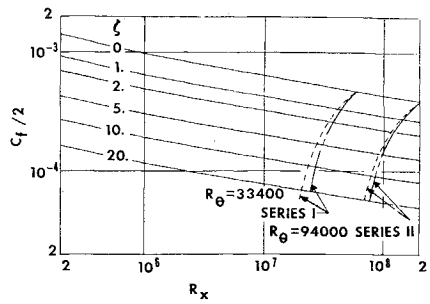

Fig. 10 Effect of transpiration on the virtual origin of the flow configuration of Ref. 17: broken lines, locus of effective Reynolds number; dashed lines, lines of constant momentum thickness Reynolds number.

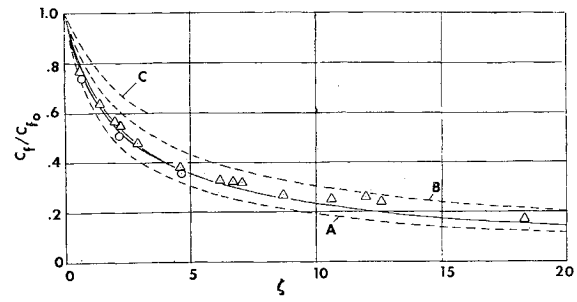

Fig. 12 Comparison of theory and experiment for high-speed homogeneous injection (M_e = 3.2, adiabatic wall): solid line, present prediction; curve A, present prediction with R_x = const.; curve B, prediction of Ref. 3; curve C, faired curve through data of Ref. 18; symbols, data of Ref. 17.

ber and wall temperature conditions. This disparity is greater than would appear from this direct comparison since the results of Ref. 18 (curve C) were obtained with a configuration where $\Delta R_x/R_{x_0} \gg 0$ which corresponds very nearly to the constant R_x case in contrast to the (almost) constant R_θ results of Ref. 17. These results would indicate that the Mach number effect indicated by the data of Ref. 18 is illusory, at least insofar as reduction of *local* skin friction due to transpiration. In this connection additional calculations were generated over a range of Mach number from 1.0 to 4.3 and virtually no Mach number effect was observed.[11]

Ablation and Combustion of a Graphite Cylinder

The applicability of this formulation to a configuration involving chemical reaction was examined in Ref. 19 and the predictions compared with the data obtained by Denison.[5] Here the test item consisted of a graphite cylinder forming part of a blowdown system which could provide a controlled mixture of oxygen and nitrogen as the tunnel fluid. The cylinder was preheated inductively to a temperature of approximately 3000°F. The subsequent flow of oxidizing gas over the hot graphite caused ignition and further heating, by virtue of combustion, to some equilibrium temperature which varied according to the external concentration and pressure level. These temperatures were determined experimentally by employing a radiamatic pyrometer. In addition, the instantaneous surface recession was obtained by means of a specially designed x-ray system.

In order to derive the required energy and species solutions for this case, Crocco integral variations were assumed for total enthalpy and element mass fractions. Then, if a flame sheet model for combustion is adopted and due account is taken of the environmental conditions of the tests it is found that¶ 1) the flame sheet coincides with the surface $y = 0$, 2) the blowing parameter ζ is related to the external mass fraction of oxygen by $\zeta = (\frac{8}{4})Y_{O_{2e}}$, 3) the prevailing molecular species include only CO, O_2, and N_2, and are related to the velocity distribution by

$$Y_{CO} = \tfrac{7}{3}\zeta(1 - \tilde{u})/(1 + \zeta)$$

$$Y_{O_2} = Y_{O_{2e}}\tilde{u}$$

$$Y_{N_2} = Y_{N_{2e}}(1 + \zeta\tilde{u})/(1 + \zeta)$$

Integration of the working equations was then carried out using these representations with ζ maintained constant at the appropriate value yielding the variation of c_f with streamwise Reynolds number as shown in Fig. 13. From these results the steady-state ablation rate $\dot{m}_w$ was computed from the relation

$$\dot{m}_w = \zeta\rho_e u_e(c_f/2)$$

which follows from the definitions. Here the appropriate value of $c_f/2$ was determined by taking the leading edge of the cylinder to be the effective origin. The results of this calculation are compared with the experimental data and with the predictions of an earlier analysis[5] in Fig. 14. As may be seen the current prediction exhibits good agreement with the data and shows marked improvement over the earlier prediction.

V. Conclusions

The results of this study can be summarized as follows.

The feasibility of extending Coles' compressibility transformation to turbulent boundary-layer flows with mass transfer has been demonstrated, at least for the zero pressure gradient case.

Application of this method to the high-speed homogeneous case, low-speed binary case, and to a case involving the abla-

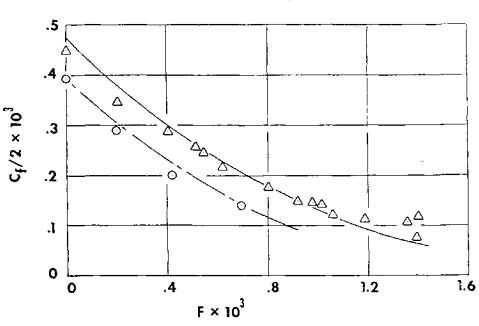

Fig. 11 Comparison of theoretical predictions for local skin friction with data of Ref. 17: triangles and solid line, series I; circles and broken line, series II, (c.f. table II).

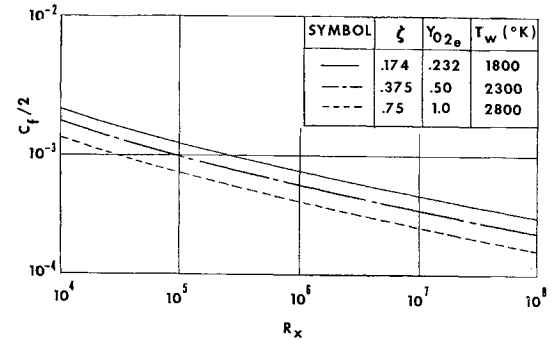

Fig. 13 Streamwise variation of local skin-friction coefficient on a graphite cylinder with ablation and equilibrium combustion as a function of surface temperature and external stream oxygen mass fraction (M_e = 0.41, T_e = 285°K).

¶ See Ref. 19 for more detailed development.

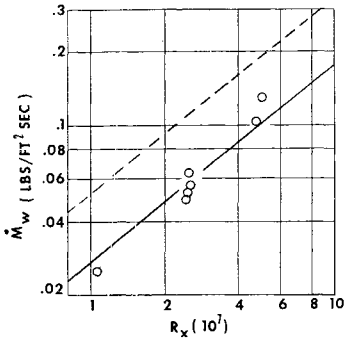

Fig. 14 Comparison of theoretical predictions for ablation rate with data of Ref. 5: solid line, present prediction; dashed line, prediction of Ref. 5; circles, data of Ref. 5 for $Y_{02e} = 1.0$.

tion and combustion of a graphite cylinder in conjunction with Crocco type integral solutions for energy and species has been shown to yield more accurate predictions for gross boundary-layer properties than those obtained using earlier analyses. This improvement can be attributed to the more realistic representation of the fluid mechanics that the transformation technique provides.

The transformation correctly maps VP velocity profiles to CP form in the inner law of the wall region. However, in complete analogy with the impermeable results of Ref. 7, the transformation distorts the "wake portion" of the profiles in the sense that the flat plate value of the Coles wake parameter Π is not recovered. The magnitude of this distortion has been shown to be roughly correlated by the density ratio ρ_w/ρ_e across the boundary layer.

References

[1] Ness, N., "Foreign Gas Injection in a Compressible Turbulent Boundary Layer on a Flat Plate," *Journal of the Aerospace Sciences*, Vol. 28, No. 8, Aug. 1961, pp. 645–654.

[2] Pappas, C. C. and Rubesin, M. W., "An Analysis of the Turbulent Boundary Layer Characteristics on a Flat Plate with Distributed Light Gas Injection," TN 4149, Feb. 1958, NACA.

[3] Rubesin, M. W., "An Analytical Estimation of the Effect of Transpiration Cooling on the Heat Transfer and Skin Friction Characteristics of a Compressible Turbulent Boundary Layer," TN 3341, Dec. 1954, NACA.

[4] Dorrance, W. H. and Dore, F. J., "The Effect of Mass Transfer on the Compressible Turbulent Boundary Layer Skin Friction and Heat Transfer," *Journal of the Aeronautical Sciences*, Vol. 21, No. 6, June 1954, pp. 404–410.

[5] Denison, M. R., "The Turbulent Boundary Layer on Chemically Active Ablating Surfaces," *Journal of the Aerospace Sciences*, Vol. 28, No. 6, June 1961, pp. 471–479.

[6] Marxman, G. A., "Combustion in the Turbulent Boundary Layer on a Vaporizing Surface," *Tenth Symposium (Intl) on Combustion*, The Combustion Institute, 1965, pp. 1337–1349.

[7] Baronti, P. O. and Libby, P. A., "Velocity Profiles in Turbulent Compressible Boundary Layers," *AIAA Journal*, Vol. 4, No. 2, Feb. 1966, pp. 193–202.

[8] Coles, D. E., "The Turbulent Boundary Layer in a Compressible Fluid," Rept. R-403-PR, Sept. 1962, Rand Corp.

[9] Stevenson, T. N., "A Law of the Wall for Turbulent Boundary Layers with Suction or Injection," Rept. 166, 1963, College of Aeronautics, Cranfield, England.

[10] Stevenson, T. N., "A Modified Velocity Defect Law for Turbulent Boundary Layers with Injection," Rept. 20, 501, 1958, Aeronautical Research Council of London, England.

[11] Economos, C., "The Compressible Turbulent Boundary Layer with Mass Transfer," Ph.D. dissertation, June 1968, Polytechnic Institute of Brooklyn.

[12] Clauser, F. H., "Turbulent Boundary Layers in Adverse Pressure Gradient," *Journal of the Aeronautical Sciences*, Vol. 21, 1954, pp. 91–108.

[13] Coles, D., "The Law of the Wake in the Turbulent Boundary Layer," *Journal of Fluid Mechanics*, Vol. 1, 1956, pp. 191–226.

[14] Smith, D. W. and Walker, J. H., "Skin Friction Measurements in Incompressible Flow," TN 4231, March 1958, NACA.

[15] Scott, C. T. et al., "Measurements of Velocity and Concentration Profiles for Helium Injection into a Turbulent Boundary Layer Flowing Over an Axial Circular Cylinder, Part I—Experimental Results," HTLTR-55, Feb. 1964, Univ. of Minnesota.

[16] Bromley, L. A. and Wilke, C. R., "Viscosity Behavior of Gases," *Industrial and Engineering Chemistry*, Vol. 43, No. 7 July 1951, pp. 1641–1648.

[17] Dershin, H., Leonard, C. A., and Gallaher, W. H., "Direct Measurement of Compressible, Turbulent Boundary Layer Skin Friction on a Porous Flat Plate with Mass Injection," *AIAA Journal*, Vol. 5, No. 11, Nov. 1967, pp. 1934–1939.

[18] Pappas, C. C. and Okuno, A. F., "Measurements of Skin Friction of the Compressible Turbulent Boundary Layer on a Cone with Foreign Gas Injection," *Journal of the Aerospace Sciences*, Vol. 27, No. 5, May 1960, pp. 321–333.

[19] Schneider, J., "Missile Phenomenology Studies," TR-684, Jan. 1968, General Applied Science Labs.

[20] Mickley, H. S. and Davis, R. S., "Momentum Transfer for Flow Over a Flat Plate with Blowing," TN 4017, 1957, NACA.